RECOVERY AND REGULARIZATION OF THE INITIAL TEMPERATURE DISTRIBUTION IN A CYLINDER

Khalid Masood, Salim Messaoudi and F.D. Zaman

Department of Mathematical Sciences

King Fahd University of Petroleum and Minerals

Dhahran 31261, Saudi Arabia

masood@kfupm.edu.sa

Abstract: We investigate the inverse problem in a circular cylinder involving recovery of the initial temperature distribution from measurements of the final temperature distribution. This problem is extremely ill-posed and it is desirable to regularize the problem to get some meaningful information. We reformulate the problem with a regularizing parameter which closely approximates and regularizes the heat conduction model.

Key Words: Invese problems, Initial Temperature, Regularization

1. Introduction

The classical direct problem in heat conduction is to determine the temperature distribution of a body as the time progresses. The task of determining the initial temperature distribution from the final distribution is distinctly different from the direct problem and it is identified as the initial inverse heat conduction problem.

The initial inverse problem based on the parabolic heat equation is extremely ill-posed; see e.g. Engl [1]. There exists an alternate approach to the initial inverse problem that consists of a complete reformulation of the governing equation. The inverse problem based upon the parabolic heat equation is closely approximated by a hyperbolic heat equation; see e.g. Weber [2], and Elden [3]. This alternate formulation gives rise to an inverse problem, which is stable and well-posed and numerical methods

for such problems are efficient and accurate. The alternate formulation has some physical advantages. In many applications, one encounters a situation where the usual parabolic heat equation does not serve as a realistic model. Since the speed of propagation of the thermal signal is finite, e.g. for short-pulse laser applications, the hyperbolic differential equation correctly models the problem; see Vedavarz et al. [4] and Gratzke et al. [5] among others. Moreover, as we see in section 3, the parabolic heat conduction model can be treated as limiting case of the hyperbolic model. We introduce a hyperbolic term with a small parameter in the parabolic heat equation and apply WKBJ method [6] to solve the direct problem by utilizing the small value of the parameter. We regularize the solution by controlling the size of the parameter and show that the solution is valid in case there is noise in the data.

In the second section we solve the inverse problem in the parabolic heat equation in a circular cylinder. In the third section the inverse problem in the hyperbolic heat equation with a small parameter is solved and compared with the inverse solution of the parabolic heat equation. An example is also presented to check the validity of the inverse solution. We perform some numerical experiments and results of these experiments are analyzed in the fourth section. Finally, in the last section results are summarized.

2. Recovery of the Initial Temperature Distribution in a Circular Cylinder

We consider a circular cylinder with radius $0 < r < a$, and height $0 < z < b$, whose temperature at the point (r, z) and at time t is given by the function $u(r, z, t)$. Then, for an appropriate choice of units, $u(r, z, t)$ satisfies the equation

$$\frac{\partial u}{\partial t} = \frac{\partial^2 u}{\partial r^2} + \frac{1}{r}\frac{\partial u}{\partial r} + \frac{\partial^2 u}{\partial z^2}, \quad t > 0, \text{ and } r, z \in R, \tag{1}$$

where R is the following region

$$R = \{(r, z) \,/\, r \in [0, a] \,,\, z \in [0, b]\}, \tag{2}$$

with homogeneous Dirichlet boundary conditions

$$u(a, z, t) = 0, \quad z \in [0, b] \,, \tag{3}$$

$$u(r, 0, t) = u(r, b, t) = 0, \quad r \in [0, a] \,. \tag{4}$$

Assume the final temperature

$$f(r, z) \doteq u(r, z, T). \tag{5}$$

Our aim is to determine the initial temperature profile $g(r, z)$

$$g(r, z) \doteq u(r, z, 0). \tag{6}$$

We assume the solution of the direct problem in the form

$$u(r, z, t) = \sum_{n,m=1}^{\infty} v_{n,m}(t)\, \phi_{n,m}(r, z) \,, \quad r, z \in R. \tag{7}$$

The solution of the corresponding eigenvalue problem is given by

$$\phi_{n,m}(r, z) \doteq \frac{2}{a\sqrt{b}J_0'(a\lambda_n)} \sin(\mu_m z)\, J_0(\lambda_n r) \,,$$

where $\mu_m = \frac{m\pi}{b}$, λ_n are solutions of $J_0(\lambda_n a) = 0$, and $\prime$ denotes derivative with respect to r. The eigenfunctions $\phi_{n,m}(r, z)$ form a complete orthonormal system in $H_r[R]$. Thus $g(r, z) \in H_r[R]$ can be expanded as

$$g(r, z) = \sum_{n,m=1}^{\infty} c_{n,m}\phi_{n,m}(r, z) \,, \quad r, z \in R, \tag{8}$$

where

3

$$c_{n,m} = \int_0^a \int_0^b \tau g(\tau, \eta) \phi_{n,m}(\zeta, \eta) d\eta d\tau. \tag{9}$$

Substitute (7) in (1) and (6), and using orthonormality property of the eigenfunctions leads to the following ordinary differential equation

$$\frac{\partial v_{n,m}(t)}{\partial t} + \left[\mu_m^2 + \lambda_n^2\right] v_{n,m}(t) = 0, \qquad t > 0, \tag{10}$$

$$v_{n,m}(0) = c_{n,m}. \tag{11}$$

This initial value problem can easily be solved and so (7) takes the form

$$u(r, z, t) = \sum_{n,m=1}^{\infty} c_{n,m} \exp\left\{-\left[\mu_m^2 + \lambda_n^2\right] t\right\} \phi_{n,m}(r, z), \quad r, z \in R. \tag{12}$$

Now we use condition (5) to write the final profile in the form

$$\begin{aligned} f(r, z) &= \sum_{n,m=1}^{\infty} c_{n,m} \exp\left\{-\left[\mu_m^2 + \lambda_n^2\right] T\right\} \phi_{n,m}(r, z), \\ &= \int_0^a \int_0^b \tau g(\tau, \eta) K(r, z, \tau, \eta) \, d\eta d\tau, \end{aligned} \tag{13}$$

where

$$K(r, z, \tau, \eta) = \sum_{n,m=1}^{\infty} \exp\left\{-\left[\mu_m^2 + \lambda_n^2\right] T\right\} \phi_{n,m}(\tau, \eta) \phi_{n,m}(r, z). \tag{14}$$

Thus the inverse problem is reduced to solving integral equation of the first kind. The singular system for the integral operator in (13) is given by

$$\left[\exp\left\{-\left[\mu_m^2 + \lambda_n^2\right] T\right\}; \quad \phi_{n,m}(r, z), \ \phi_{n,m}(r, z)\right]. \tag{15}$$

It now follows from Picard's theorem [1] that our inverse problem is solvable iff

4

$$\sum_{n,m=1}^{\infty} \frac{|f_{n,m}|^2}{\left[\exp\left\{-\left[\mu_m^2 + \lambda_n^2\right]T\right\}\right]^2} < \infty, \tag{16}$$

where

$$f_{n,m} \doteq \int_0^a \int_0^b f(\tau, \eta)\, \phi_{n,m}(\tau, \eta)\, d\eta\, d\tau, \tag{17}$$

are classical Fourier coefficients of f. In this case solution [1] is given by

$$g(r, z) = \sum_{n,m=1}^{\infty} \frac{f_{n,m}\phi_{n,m}(r, z)}{\left[\exp\left\{-\left[\mu_m^2 + \lambda_n^2\right]T\right\}\right]}. \tag{18}$$

Picard's theorem demonstrates the ill-posed nature of the problem considered. If we perturb the data by setting $f^\delta = f + \delta\phi_{n,m}$ we obtain a perturbed solution $g^\delta = g + \delta\phi_{n,m}\exp\left\{\left[\mu_m^2 + \lambda_n^2\right]T\right\}$. Hence the ratio $\left\|g^\delta - g\right\| / \left\|f^\delta - f\right\| = \exp\left\{\left[\mu_m^2 + \lambda_n^2\right]T\right\}$ can be made arbitrarily large due to the fact that the singular values $\exp\left\{-\left[\mu_m^2 + \lambda_n^2\right]T\right\}$ decay exponentially.

3. Regularizing the Inverse solution by a hyperbolic model

In order to overcome the ill-posedness of the inverse problem, we may model the problem by introducing a hyperbolic term with a small parameter in the classical heat equation. It is well established that this new model regularizes the problem in classical heat model, see e.g. Masood et. al. [7]. We consider the two dimensional hyperbolic heat equation with small parameter ϵ as follows:

$$\epsilon\frac{\partial^2 u}{\partial t^2} + \frac{\partial u}{\partial t} = \frac{\partial^2 u}{\partial r^2} + \frac{1}{r}\frac{\partial u}{\partial r} + \frac{\partial^2 u}{\partial z^2}, \qquad \epsilon, t > 0, \ \ and \ \ r, z \in R, \tag{19}$$

where the parameter ϵ is assumed to be small and $\epsilon \to 0^+$ and R is the region (2). Together with conditions $(3) - (6)$ and one additional condition given below

$$\frac{\partial u}{\partial t}(r, z, 0) = 0. \tag{20}$$

5

The problem (19) together with $(3) - (6)$ and (20) can be solved by the method described in the previous section. Assume solution of the form (7), which in this case leads to the following initial value problem

$$\epsilon \frac{\partial^2 v_{n,m}(t)}{\partial t^2} + \frac{\partial v_{n,m}(t)}{\partial t} + \left[\mu_m^2 + \lambda_n^2\right] v_{n,m}(t) = 0, \qquad t > 0, \tag{21}$$

$$v_{n,m}(0) = c_{n,m}, \tag{22}$$

$$\frac{d}{dt} v_{n,m}(0) = 0. \tag{23}$$

Since $\epsilon \to 0^+$, this is a singular perturbation problem. We apply the WKBJ method [6] to obtain an asymptotic representation for the solution of (21) containing parameter ϵ; the representation is to be valid for small values of the parameter. It is demonstrated in [6] that the solution stays closer to the exact solution for large values such as $\epsilon = 0.5$. The solution of (21) is given by

$$\begin{aligned}
v_{n,m}(t) &= \left\{ \frac{\left(\mu_m^2 + \lambda_n^2 - \frac{1}{\epsilon}\right) c_{n,m}}{2\left(\mu_m^2 + \lambda_n^2\right) - \frac{1}{\epsilon}} \right\} \exp\left\{ -\left(\mu_m^2 + \lambda_n^2\right) t \right\} \\
&\quad + \left\{ \frac{\left(\mu_m^2 + \lambda_n^2\right) c_{n,m}}{2\left(\mu_m^2 + \lambda_n^2\right) - \frac{1}{\epsilon}} \right\} \exp\left\{ \left(\mu_m^2 + \lambda_n^2\right) t - \frac{t}{\epsilon} \right\}.
\end{aligned} \tag{24}$$

Now we use condition (5) to write the final profile in the form

$$\begin{aligned}
f(r,z) &= \sum_{n,m=1}^{\infty} \left[\left\{ \frac{\left(\mu_m^2 + \lambda_n^2 - \frac{1}{\epsilon}\right) c_{n,m}}{2\left(\mu_m^2 + \lambda_n^2\right) - \frac{1}{\epsilon}} \right\} \exp\left\{ -\left(\mu_m^2 + \lambda_n^2\right) T \right\} \right. \\
&\quad \left. + \left\{ \frac{\left(\mu_m^2 + \lambda_n^2\right) c_{n,m}}{2\left(\mu_m^2 + \lambda_n^2\right) - \frac{1}{\epsilon}} \right\} \exp\left\{ \left(\mu_m^2 + \lambda_n^2\right) T - \frac{T}{\epsilon} \right\} \right] \phi_{n,m}(r,z), \\
&= \int_0^a \int_0^b g(\tau,\eta) K(x,y,\tau,\eta)\, d\eta d\tau, \tag{25}
\end{aligned}$$

where

$$
\begin{aligned}
K\left(r, z, \tau, \eta\right) \quad = \quad & \sum_{n,m=1}^{\infty} \left[\left\{ \frac{\mu_m^2 + \lambda_n^2 - \frac{1}{\epsilon}}{2\left(\mu_m^2 + \lambda_n^2\right) - \frac{1}{\epsilon}} \right\} \exp\left\{ -\left(\mu_m^2 + \lambda_n^2\right) T \right\} + \left\{ \frac{\left(\mu_m^2 + \lambda_n^2\right)}{2\left(\mu_m^2 + \lambda_n^2\right) - \frac{1}{\epsilon}} \right\} \right. \\
& \left. \exp\left\{ \left(\mu_m^2 + \lambda_n^2\right) T - \frac{T}{\epsilon} \right\} \right] \phi_{n,m}(\tau, \eta)\phi_{n,m}(r, z).
\end{aligned} \tag{26}
$$

Thus the inverse problem is reduced to solving integral equation of the first kind. The singular system for the integral operator in (25) is given by

$$
\left[\begin{array}{c} \left\{ \dfrac{\mu_m^2 + \lambda_n^2 - \frac{1}{\epsilon}}{2\left(\mu_m^2 + \lambda_n^2\right) - \frac{1}{\epsilon}} \right\} \exp\left\{ -\left(\mu_m^2 + \lambda_n^2\right) T \right\} \\[4mm] + \left\{ \dfrac{\mu_m^2 + \lambda_n^2}{2\left(\mu_m^2 + \lambda_n^2\right) - \frac{1}{\epsilon}} \right\} \exp\left\{ \left(\mu_m^2 + \lambda_n^2\right) T - \dfrac{T}{\epsilon} \right\}; \qquad \phi_{n,m}(r, z), \ \ \phi_{n,m}(r, z) \end{array} \right] \tag{27}
$$

It now follows from Picard's theorem that our inverse problem is solvable iff

$$
\sum_{n,m=1}^{\infty} \frac{|f_{n,m}|^2}{\left[\left\{ \dfrac{\mu_m^2 + \lambda_n^2 - \frac{1}{\epsilon}}{2\left(\mu_m^2 + \lambda_n^2\right) - \frac{1}{\epsilon}} \right\} \exp\left\{ -\left(\mu_m^2 + \lambda_n^2\right) T \right\} + \left\{ \dfrac{\mu_m^2 + \lambda_n^2}{2\left(\mu_m^2 + \lambda_n^2\right) - \frac{1}{\epsilon}} \right\} \exp\left\{ \left(\mu_m^2 + \lambda_n^2\right) T - \dfrac{T}{\epsilon} \right\} \right]^2} < \infty, \tag{28}
$$

where $f_{n,m}$ are classical Fourier coefficients of f given by expression (17). In this case solution is given by

$$g(r, z) = \sum_{n,m=1}^{\infty} \frac{f_{n,m}\phi_{n,m}(r, z)}{\left[\left\{\dfrac{\mu_m^2+\lambda_n^2-\dfrac{1}{\epsilon}}{2\left(\mu_m^2+\lambda_n^2\right)-\dfrac{1}{\epsilon}}\right\} \exp\left\{-\left(\mu_m^2+\lambda_n^2\right)T\right\} + \left\{\dfrac{\mu_m^2+\lambda_n^2}{2\left(\mu_m^2+\lambda_n^2\right)-\dfrac{1}{\epsilon}}\right\} \exp\left\{\left(\mu_m^2+\lambda_n^2\right)T-\dfrac{T}{\epsilon}\right\}\right]}. \tag{29}$$

Letting $\epsilon \to 0^+$, in (28) and (29), we see that it approaches to the solution given by (16) and (18). This shows that the parabolic heat conduction model can be treated as a limiting case of the hyperbolic heat conduction model. It is shown in [7] that by choosing an appropriate value of the parameter ϵ the hyperbolic heat conduction model behaves much better than the parabolic heat conduction model.

Example: Consider

$$g(r, z) = \frac{2}{a\sqrt{a}J_0'(a\lambda_n)} \sin\left(\mu_m z\right) J_0(\lambda_m r) = \phi_{m,m}(r, z), \text{ with } a = b. \tag{30}$$

First step is to solve the direct problem. The final profile $f(x, y)$ for the heat equation and the hyperbolic heat equation can be calculated from the expression (13) and (25) respectively. The resulting expressions are used in (17) to get the Fourier coefficients. The Fourier coefficients (in the case, $m = n$) for hyperbolic heat equation are

$$f_{m,m} = \frac{\left(\mu_m^2 + \lambda_m^2\right)\epsilon - 1}{2\left(\mu_m^2 + \lambda_m^2\right)\epsilon - 1} \exp\left[-\left(\mu_m^2 + \lambda_m^2\right)T\right] + \frac{\left(\mu_m^2 + \lambda_m^2\right)\epsilon}{2\left(\mu_m^2 + \lambda_m^2\right)\epsilon - 1} \tag{31}$$
$$\exp\left[\left(\mu_m^2 + \lambda_m^2\right)T - \frac{T}{\epsilon}\right],$$

and for the parabolic heat equation

$$f_{m,m} = \exp\left[-\left(\mu_m^2 + \lambda_m^2\right)T\right]. \tag{32}$$

Finally using the data given by (31) and (32) in (29) and (18) respectively, we see that the recovered initial profile is given by (30).

4. Numerical Experiments

We analyze the models by adding white Gaussian noise to the data (32) and setting $a = 8$. In Figs. 2−3 and 5−8, we use the noisy data (white Gaussian noise+(32)) in both parabolic heat conduction and hyperbolic heat conduction models and see the mean behavior of 100 independent realizations. To study the behavivior of models, only a small crossection of the initial profile is analysed.

The exact initial profile is shown in the Fig. 1 for $m = 2$. We have considered the second mode, that is, $m = 2$ in Figs. 2−3. Also we have retained first three terms ($N = 3$) in series (18) and (29) and time displacement $T = 1$. The method of truncating the series after first few terms [8] is called truncated singular value decomposition (TSVD). In Figs. 2−3, the signal to noise ratio (SNR) is equal to 20 dB. It is clear from the comparison fig.2 and Fig. 3 that the hyperbolic heat conduction model behaves better than the parabolic heat conduction model for $\epsilon = 0.01$.

The exact initial profile in the case $m = 4$ is shown in the Fig. 4. In Figs. 5−6, we have considered $m = 4$, $N = 4, T = 1$ and $SNR = 20dB$. We observe the behavior of the parabolic heat conduction model in Fig. 6, noting the range of the vertical axis. However for the hyperbolic model in Fig. 5 with $\epsilon = 0.02$, the recovered profile is almost the exact initial profile. So, from the above analysis of figures, we conclude that the hyperbolic model behaves much better than the parabolic heat conduction model in the case of noisy data. Even for lower modes, if the magnitude of noise increases, the parabolic heat conduction model becomes highly unstable.

The same analysis applies to further higher modes. To see the effects of the size of parameter T in both models, we set $T = 2$ in Figs. 7−8. Comparing Figs. 7−8 with Figs. 2−3. For the parabolic heat conduction model, there is large degradation. However, for the hyperbolic model, there is a little degradation. This behavior is due

9

the faster rate of decay of singular values for larger time displacement. The same analysis will apply to the size of a, the rate of decay of singular values will be faster for smaller a and vice versa.

To choose ϵ, we start from a higher value of ϵ for which there is no spikes appearing on the graph. We gradually reduce the size and note the values of ϵ for which the spikes start to appear. We reduce the size further and note the values of ϵ for which the spikes amplify significantly. Then we take the mean of the two values of ϵ, which will give an appropriate choice of ϵ. This choice of ϵ may be refined further by checking neighboring values for which the spikes are milder.

Conclusions

The inverse solution of the heat conduction model is characterized by discontinuous dependence on the data. A small error in the nth Fourier coefficient is amplified by the factor $\exp\left\{\left(\mu_m^2 + \lambda_n^2\right) T\right\}$. Thus it depends on the rate of decay of singular values and this rate of decay also depends on the size of the parameter T, a and b. In order to get some meaningful information, one has to consider first few degrees of freedom in the data and has to filter out everything else depending on the rate of decay of singular values and the size of parameter T. It is possible to recover information about the higher modes by the proposed hyperbolic model.

It is shown that a complete reformulation of the heat conduction problem as a hyperbolic equation produces meaningful results. The hyperbolic model with a small parameter closely approximates and regularizes the heat conduction equation. It is also shown that in case of noisy data, the hyperbolic model approximates the exact initial profile better than the parabolic heat conduction model. Further, in the case of noisy data, the information about the initial profile cannot even be recovered for higher modes by the parabolic heat conduction model but the hyperbolic model may give some useful information about the initial profile if the value of parameter ϵ is

chosen appropriately.

Acknowledgment:

References

[1] H. W. Engl, Martin Hanke and Andreas Neubauer, Regularization of Inverse Problems, Kluwer, Dordrecht, 1996, pp. 31-42.

[2] C. F. Weber, Analysis and solution of the ill-posed problem for the heat conduction problem, International Journal of Heat and Mass Transfer 24 (1981) 1783-1792.

[3] L. Elden, Inverse and Ill-Posed Problems, (H. W. Engl and C. W. Groetsch, eds.), Academic Press, Inc. 1987, pp. 345-350.

[4] A. Vedavarz, K. Mitra and S. Kumar, Hyperbolic temperature profiles for laser surface interactions, J. Appl. Phys. 76(9) (1994) 5014-5021.

[5] U. Gratzke, P. D. Kapadia and J. Dowden, Heat conduction in high-speed laser welding, J. Phys. D: APPL. Phys. 24 (1991) 2125-2134.

[6] C. M. Bender and S. A. Orszag, Advanced Mathematical Methods for Scientists and Engineers, McGraw Hill, New York, 1978.

[7] K. Masood, S. Messaoudi and F. D. Zaman, Initial Inverse Problem in Heat Equation with Bessel Operator, Int. Journal of Heat and Mass Transfer, 45(14), (2002) pp. 2959-2965.

[8] P. C. Hansen, Rank-Deficient and Discrete Ill-Posed Problems. Numerical Aspects of Linear Inversion, SIAM, 1997.
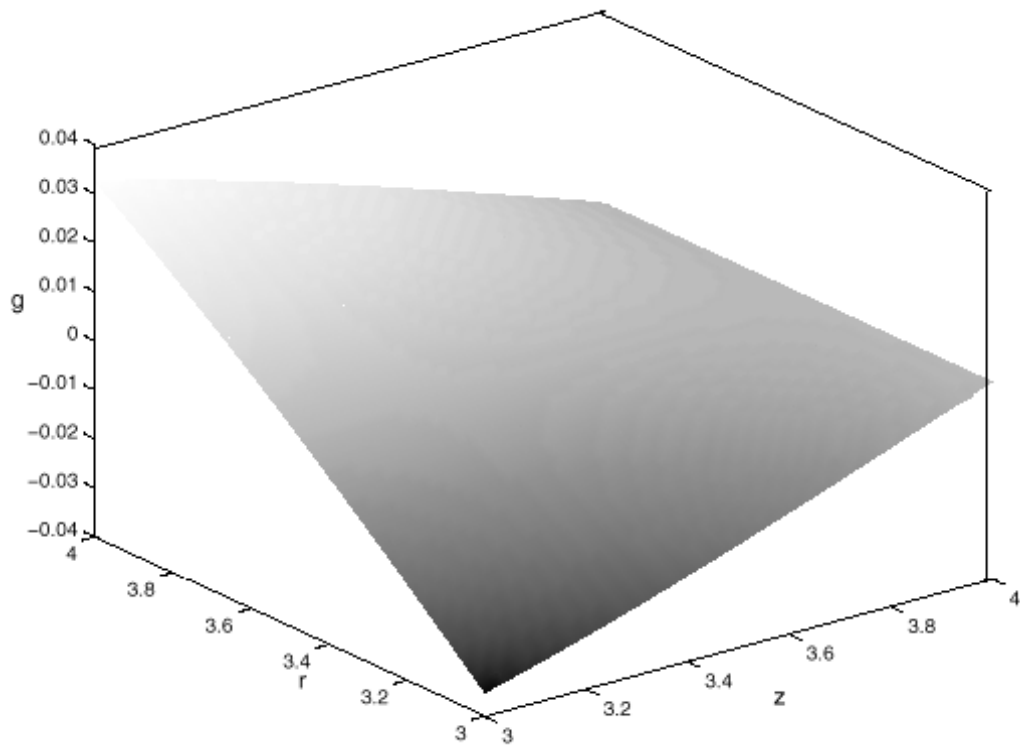
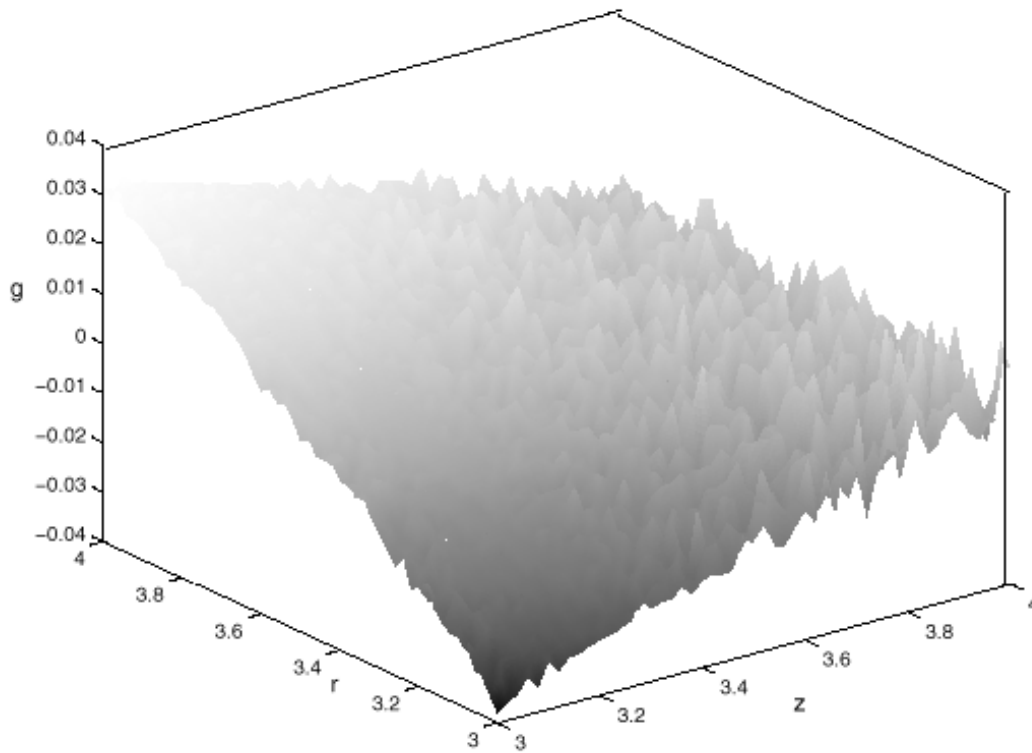FIG. 1. The exact initial profile for $m = 2$.

FIG. 2. Response of the hyperbolic model for $m = 2, T = 1, N = 3, SNR = 20dB$ and $\epsilon = 0.01$.
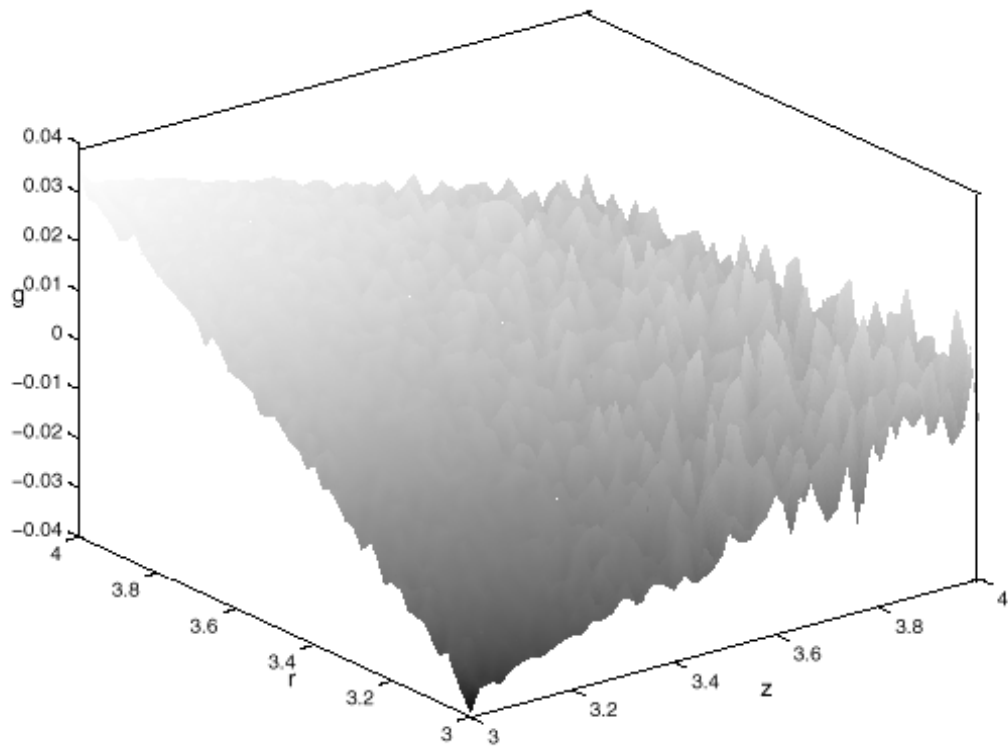
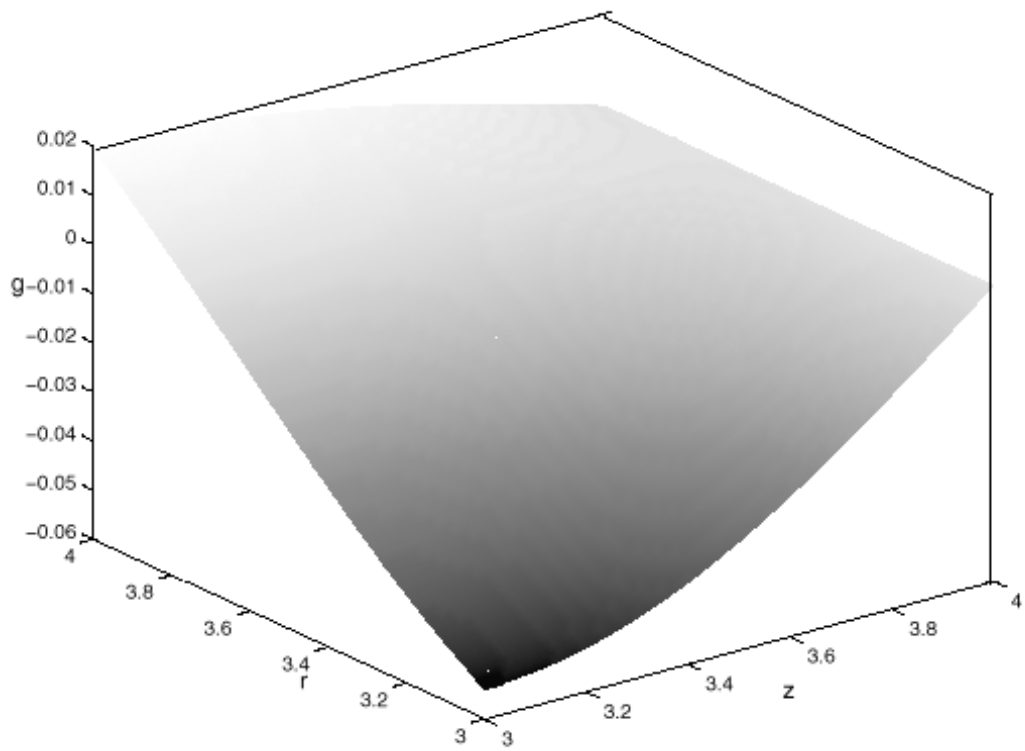FIG. 3. Response of the parabolic model for $m = 2, T = 1, N = 3$ and $SNR = 20dB$.

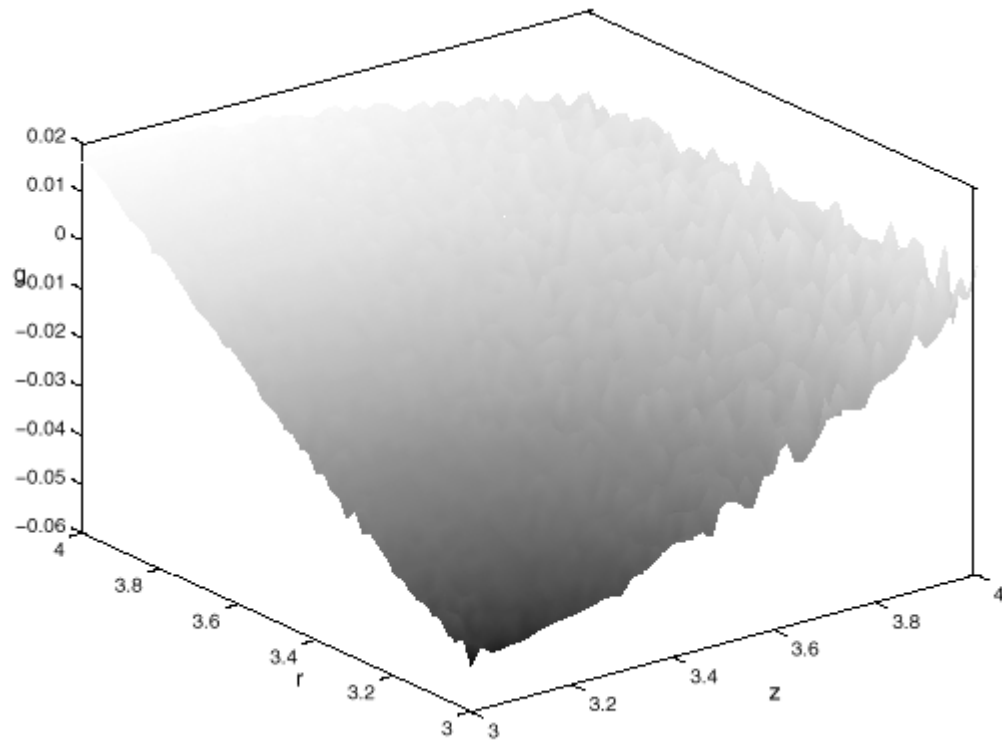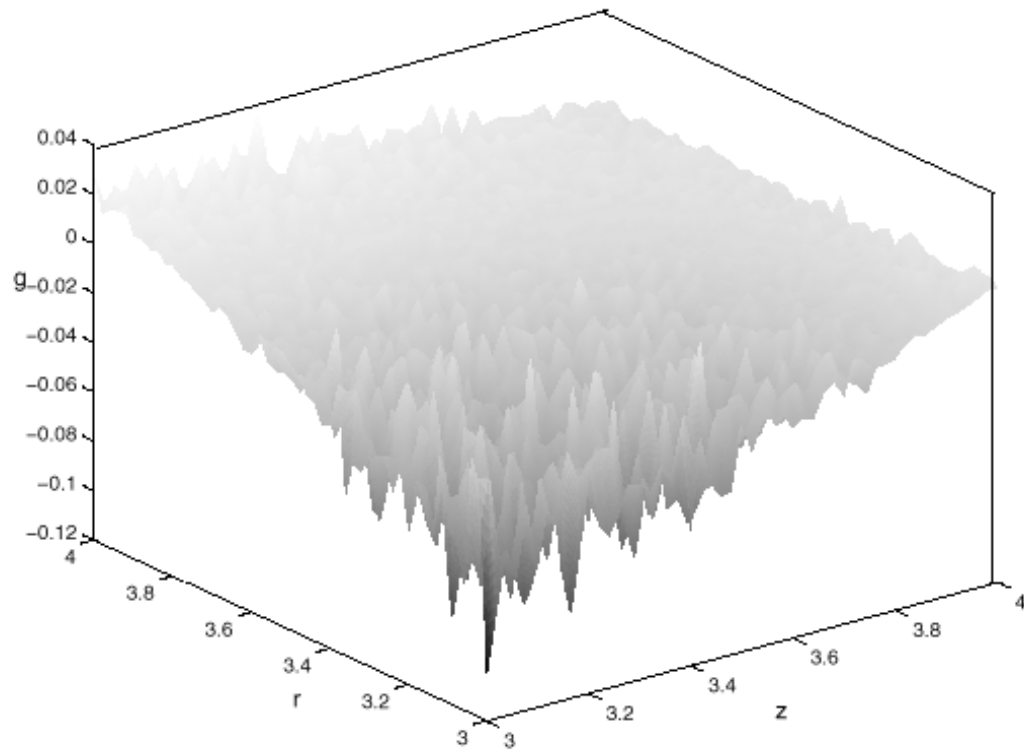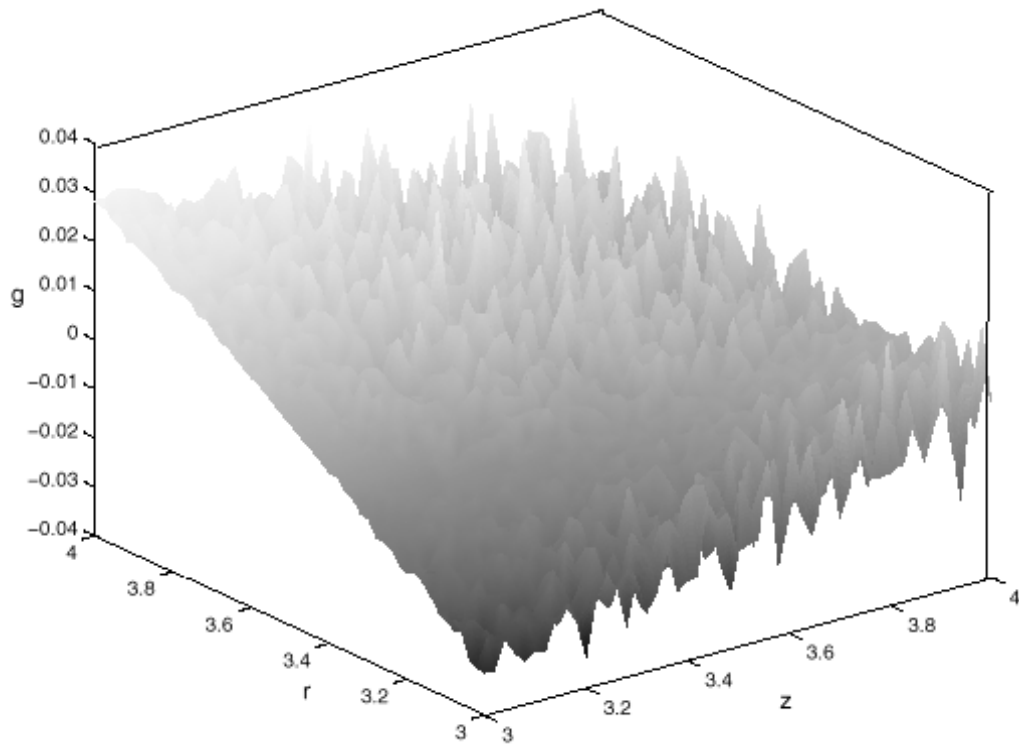FIG. 4. The exact initial profile for $m = 4$.

FIG. 5. Response of the hyperbolic model for $m = 2, T = 1, N = 4, SNR = 20dB$ and $\epsilon = 0.02$.

FIG. 6. Response of the parabolic model for $m = 2, T = 1, N = 4$ and $SNR = 20dB$.

FIG. 7. Response of the hyperbolic model for $m = 2, T = 2, N = 3, SNR = 20dB$ and $\epsilon = 0.1$.
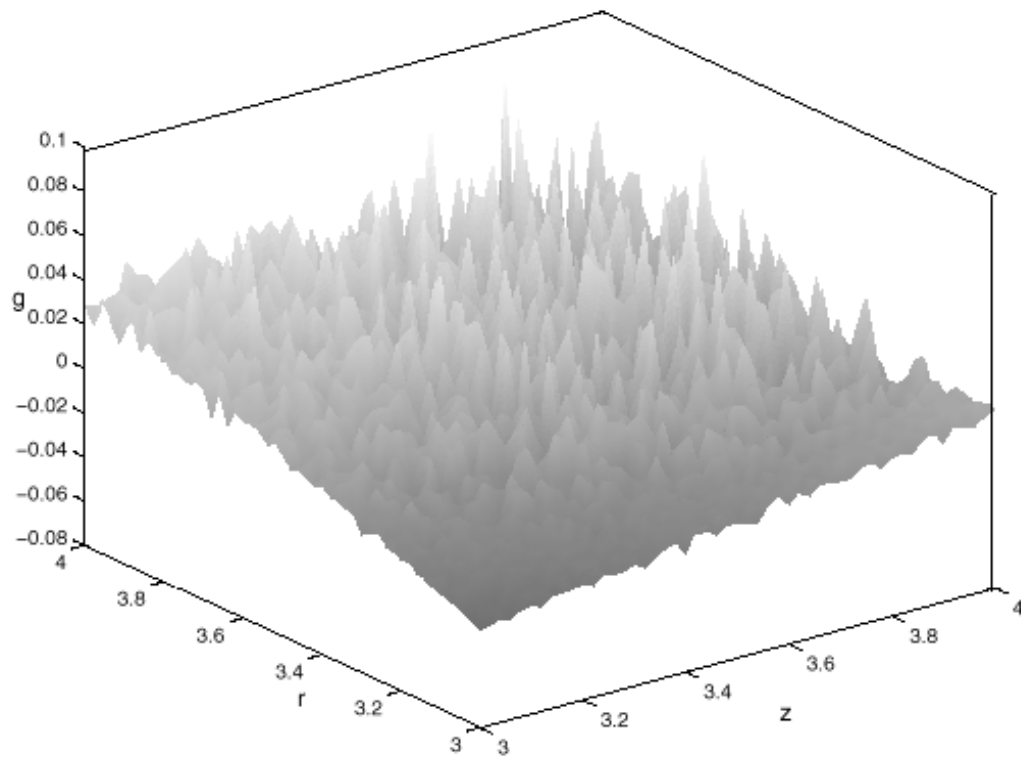
FIG. 8. Response of the parabolic model for $m = 2, T = 2, N = 3$ and $SNR = 20dB$.